



Inhibition of bacterial growth on zirconia abutment with a helium cold atmospheric plasma jet treatment

Yang Yang¹ · Miao Zheng² · Yang Yang¹ · Jing Li³ · Yong-Fei Su⁴ · He-Ping Li⁵ · Jian-Guo Tan¹

Received: 27 August 2019 / Accepted: 19 December 2019 / Published online: 15 January 2020
© Springer-Verlag GmbH Germany, part of Springer Nature 2020

Abstract

Objectives This study presents a surface modification method to treat the zirconia implant abutment materials using a helium cold atmospheric plasma (CAP) jet in order to evaluate its efficacy on oral bacteria adhesion and growth.

Materials and methods Yttrium-Stabilized Zirconia disks were subjected to helium CAP treatment; after the treatment, zirconia surface was evaluated using scanning electron microscopy, a contact angle measuring device, X-ray photoelectron spectroscopy for surface characteristics. The response of *Streptococcus mutans* and *Porphyromonas gingivalis* on treated surface was evaluated by a scanning electron microscopy, MTT assay, and LIVE/DEAD staining. The biofilm formation was analyzed using a crystal violet assay.

Results After the helium CAP jet treatment, the zirconia surface chemistry has been changed while the surface topography remains unchanged, the bacterial growth was inhibited, and the biofilm forming decreased. As the treatment time increases, the zirconia abutment showed a better bacterial inhibition efficacy.

Conclusions The helium CAP jet surface modification approach can eliminate bacterial growth on zirconia surface with surface chemistry change, while surface topography remained.

Clinical relevance Soft tissue seal around dental implant abutment plays a crucial role in maintaining long-term success. However, it is weaker than periodontal barriers and vulnerable to bacterial invasion. CAP has a potential prospect for improving soft tissue seal around the zirconia abutment, therefore providing better esthetics and most of all, prevent peri-implant lesions from happening.

Keywords Zirconia · Surface modification · Cold atmospheric plasma · Bacterial inhibition · Implant interface

Yang Yang and Miao Zheng contributed equally to this work.

✉ He-Ping Li
liheping@tsinghua.edu.cn

✉ Jian-Guo Tan
kqtanjg@bjmu.edu.cn

¹ Department of Prosthodontics, Peking University School and Hospital of Stomatology & National Clinical Research Center for Oral Diseases & National Engineering Laboratory for Digital and Material Technology of Stomatology & Beijing Key Laboratory of Digital Stomatology, Beijing 100081, People's Republic of China

² Department of Stomatology, Peking University Third Hospital, Beijing 100191, People's Republic of China

³ Department of Engineering Physics, Tsinghua University, Beijing 100084, People's Republic of China

⁴ College of Mechanical Engineering, North China University of Science and Technology, Tangshan 063210, People's Republic of China

⁵ Department of Engineering Physics, Tsinghua University, Beijing 100084, People's Republic of China

Introduction

Dental implants have been used for decades and is considered a good strategy to restore missing teeth. The soft tissue around dental implant abutment plays a critical role in the treatment process: other than providing esthetics, it also acts as a barrier against complicated oral environment, especially bacterial infections, therefore protecting underlying bones from loss and maintaining the long-term stability of implant [1]. Unfortunately, unlike soft tissue around natural teeth which have sophisticated arrangements, those around implant abutment merely forms a thin connective tissue layer with fibers paralleling to the implant [2], therefore creating a relatively weaker barrier. Such soft tissue seal could be easily disrupted and would lead to bacteria penetration, causing focal infection and bone loss, compromising the long-term success of implants. Peri-implant lesions such as peri-implantitis and peri-implant mucositis, generally known as bacterial-derived diseases

with a growing prevalence rate, still remains challenging to treat nowadays [3]. Under different diagnosis criteria, the prevalence rate of these peri-implant lesions varies. However, a general of 18.5% patients and 12.8% implants suffer from peri-implantitis, while the number on peri-implant mucositis is even higher [4]. As treatment of peri-implant lesions remains challenging, early establishment of strong and effective peri-implant soft tissue seals provides a solution to the management of the disease on a preventive scope [5].

As the quality of soft tissue around the implant abutment influences both the esthetic and function of implants [6], it can be determined by the race for the surface between host tissue cells and bacteria in the early phase of soft tissue wound healing [7]. After the implant placement, the adhesion of epithelial and connective tissue components to the abutment material processes at a relatively slow speed, while bacteria attachment starts minutes after the pellicle formed on the abutment surface [8]. Moreover, since microorganisms are frequently introduced on an implant surface during surgery process, microorganisms have a head start in this race game [9]. Two different adhesion models of host tissue cells and bacteria have been widely studied and elaborated in the previous studies [10–12]. Briefly, if the bacteria win the race for the most of the surface, it will be difficult for tissue cells to form an intact barrier, which will be more easily destructed at later stage. *Streptococcus mutans* (*S. mutans*) commonly exists in oral cavity and is one of the early colonizers to the implant abutments. Moreover, early adhesion of red complex pathogen [13] *Porphyromonas gingivalis* (*P. gingivalis*) will further weaken the soft tissue barrier, and even contribute to early implant failure. Eliminating bacterial growth in the early phase would create a better scenario for soft tissue seal, contributing to the long-term success of implant.

The effectiveness of different implant materials has been widely investigated in terms of soft tissue and bacterial response [14–17]. Titanium is a traditional material commonly used for abutments due to its remarkable mechanical properties and biocompatibility. However, a recent review believed that metallic particles of titanium might have a connection with biofilm formation [18]. In addition, the metallic color of titanium abutment makes it undesirable to be used in anterior region for esthetic concerns. As ceramic material is developing rapidly, zirconium oxide (zirconia) has been introduced as a promising material. The biocompatibility of zirconia abutment has been carefully studied comparing to titanium, and the result shows the same effectiveness [19–22]. In addition, its ivory color makes it suitable as implant abutments due to esthetic concerns, especially in the anterior region. Up to now, there are several commercially available zirconia

abutments in the market. However, as a bioinert material, it is necessary to find possible ways to enhance cell response on zirconia.

The methods of enhancing soft tissue cell response on zirconia, in order to promote soft tissue seal, have been extensively studied [23–25]. However, most studies did not consider the method's influence on oral microorganisms. The ideal abutment material surface should aim bi-functional: discouraging bacterial adhesion and growth, while encouraging tissue cell adhesion and spreading. Nevertheless, there seems to be a contradiction between promoting soft tissue cells and dis-promoting bacterial growth. Such method of meeting two requirements has been scarcely reported.

Recently, studies on plasma technology in surface modification of dental biomedical materials have been reported [26–29]. Plasma, as a partially ionized gas and the fourth state of matter, has played effective role in increasing surface wettability as well as killing variety of pathogens. The cold atmospheric plasma (CAP), which is generated at atmospheric pressure with the gas temperature close to the human body, has a promising potential in the life science field. In the last decades, plasma has been used in decontamination of heat-sensitive medical devices as well as fresh produces [30]. Mechanistically, the microbes are inactivated mainly by the reactive oxygen and nitrogen species (RONS) in CAPs [31]. However, the current studies mainly focus on bacteria inactivation [32], while the bacterial response on CAP-treated surface not fully revealed. Up to now, only several studies reported the antibacterial effect of CAP on titanium and its alloys [33–36]. For instance, a recent study found that bacterial adhesion and biofilm formation are significantly lower on CAP-treated titanium surfaces [37]. Moreover, some other studies demonstrated that CAP is able to promote host tissue cell growth [38, 39]. Taken together, CAP may facilitate the development of a bi-functional titanium surface. Zirconia, yet different with titanium in many ways, needs to be further investigated in terms of bi-functional possibility with CAP treatment. A previous study of our team [40] has proved that after CAP treatment, surface wettability of zirconia increased, human gingival fibroblast growth on zirconia enhanced, and topography remained unchanged, which indicates the potential CAP surface modification on zirconia. To further facilitate CAP usage in implantology, the bacterial response on this treated surface needs to be further investigated.

In this study, we investigated the effect of a helium CAP jet treatment on bacterial inhibition on zirconia, as a possible method for promoting peri-implant soft tissue seals during the early phase of wound healing. The gram-positive bacteria *Streptococcus mutans* and gram-negative bacteria *Porphyromonas gingivalis* were examined. The bacteria adhesion, morphology, viability, and biofilm formation ability were evaluated in vitro.

Material and methods

Sample preparation

A power analysis was estimated from a pilot study. Sample size was calculated by setting the effect size $f=2.18$, error probability $\alpha=0.05$, and power=0.95. Total sample size was 12 in each test. Yttrium-stabilized zirconia disks 15 mm diameter and 2 mm thick (Wieland, Pforzheim, Germany) were obtained using computer-aided design and computer-aided manufacturing (CAD-CAM) process. The disks were wet-polished using SiC abrasive paper till 2000-grit to a unified roughness of 0.1 μm . Before CAP treatment, specimens were ultrasonically cleaned using absolute ethanol and deionized water each for 20 min. The specimens were naturally dried and stored in room temperature for surface treatment. Disks were divided into four groups according to the plasma treating time, in which three experimental groups were treated by plasma for 30, 60, or 90 s and one group left untreated as control.

Helium CAP jet In this study, an atmospheric-pressure dielectric-barrier-discharge (AP-DBD) plasma generator was employed for the surface modification of the zirconia disks. The schematic of this device, CAP Med-I, is shown in Fig. 1. Developed by the Plasma Health Sciencetech Group (PHSG) of Tsinghua University, this device consists an AP-DBD plasma jet generator, and a main part for controlling the discharge voltage, driving frequency of the high-voltage alternating-current (HVAC) power supply, and helium flow rate. A detailed description on CAP Med-I can be referred to former study [41]. In this study, the cold plasma jet was generated with high-purity helium (13.5 slpm) as the plasma-forming gas under the discharge voltage of 2.85 kV and the frequency of 17 kHz. Prior to the CAP treatment, a helium gas with the same flow rate was admitted into the plasma generator for more than 1 min in order to flush the air out of the discharge space between electrodes. The zirconia disk was placed on the

sample stage co-axially with the geometrical axis of the plasma jet. The distance between the nozzle exit of the plasma generator and the zirconia disk surface was kept at 1.0 cm, while the disk was fixed and treated by the helium CAP jet under a preset time duration. An infrared thermometer (HTD8818D, Cofoe, Hunan, China) was used to determine the zirconia surface temperature after CAP treatment. An optical emission spectroscopy (AvaSpec, Avantes, Apeldoorn, Netherlands) was used to identify the existence of the excited species in the plasma jet region.

Surface analysis

Surface topography

The surface topography of zirconia disks was examined using field emission scanning electron microscopy (FE-SEM; S-4800 and S-8010, Hitachi, Tokyo, Japan).

Surface wettability

The surface wettability was determined using contact-angle-measuring device (OCA15Pro, Dataphysics, Filderstadt, Germany). The contact angle measurements were made at five different locations on each disk 3 s after application of a 1- μl deionized water droplet.

Surface chemical composition

The surface chemical composition was measured through X-ray photoelectron spectroscopy (XPS; Quantera SXM, ULVAC-PHI, Kanagawa, Japan) which was operated using monochromatic Al (Al $K\alpha$ line: 1486.6 eV) radiation with a spot diameter of 200 μm . Survey scan and detailed scan spectra were set at pass energy at 280 eV (step size 1.0 eV) and 55 eV (step size 0.1 eV). The binding energies for all spectra were calibrated using C1s peak (284.6 eV).

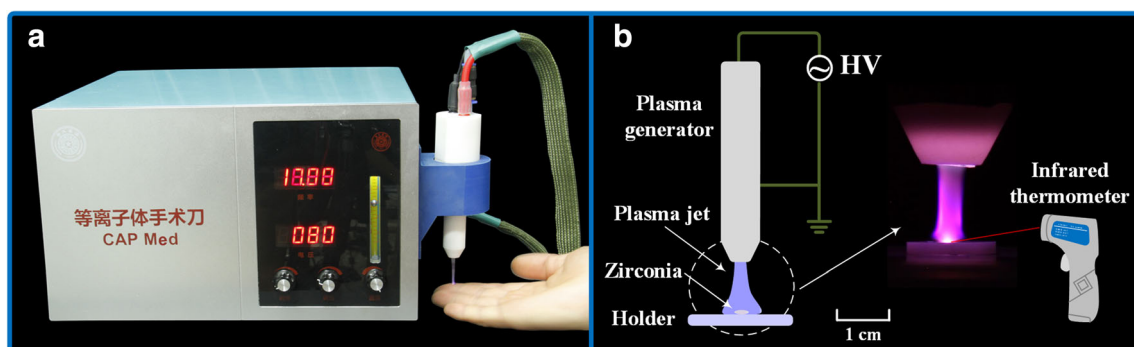


Fig. 1 Schematic of experimental setup for helium AP-DBD plasma materials treatment

Bacterial response

Bacteria culture

Gram-positive bacteria *S. mutans* (UA159) and gram-negative bacteria *P. gingivalis* (ATCC 33277) were used in this study. Bacteria were purchased from Institute of Microorganisms, Chinese Academy of Science. The pure bacteria were maintained on a brain-heart infusion (BHI) agar plate (Difco, MI, USA). The *S. mutans* were incubated under standard cell condition (5% CO₂, 95% humidified air, at 37 °C), while *P. gingivalis* was incubated under standard anaerobic condition (80% N₂, 10% H₂, 10%CO₂, at 37 °C). A monoclonal colony was transferred to 10 ml of BHI broth culture medium and let grow to exponential phase. Prior to the experiments, bacterial cells were centrifuged at 3000×g for 15 min. The bacterial pellet was washed twice with 0.1 M PBS buffer (Solarbio, Beijing, China) and suspended again, adjusted to different final concentration accordingly. Before seeding, the suspensions were shaken 30 s (Vortex 2, IKA, Staufen, Germany) in order to get single cells or pairs, then seeded on the sterilized samples in 24-well plate for further experiments. Each experiment was repeated on three separate occasions.

Bacterial adhesion assay (MTT colorimetric assay)

The MTT colorimetric assay is based on the cleavage of MTT into a blue formazan by living cell enzymes. The amount of formazan formed is correlated to the total number of viable cells. The MTT assay was performed as previously described [42]. Briefly, the MTT solution was prepared by dissolving 5 mg/ml MTT (3-(4,5-dimethylthiazol-2-yl)-2,5-diphenyltetrazolium bromide, Biosynth, IL, USA) in PBS buffer. The

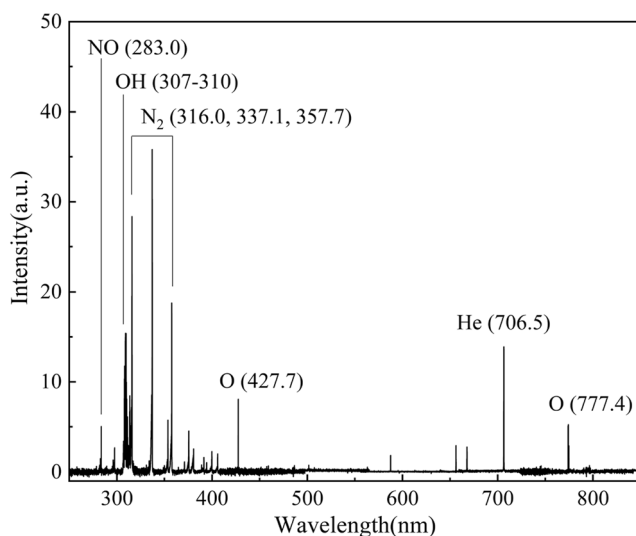


Fig. 2 Optical emission spectrum from jet region of helium AP-DBD plasma

bacteria with final concentration of 1×10^8 CFU/ml were cultivated on zirconia disks for 24 h, 48 h, and 72 h. After the culture medium removed, the cells were washed three times with sterile PBS solution to remove non-attached cells. Five microliters MTT solution and 500 μ l BHI broth culture medium were added on the disks and incubated at standard cultivation condition for 3 h in the dark. The formazan crystals formed in viable cells were dissolved by 500 μ l DMSO (ThermoFisher Scientific, MA, USA). The optical density of the solution was determined at 570 nm using a microplate reader (ELX808, BioTek, VT, USA). Experiments of all four groups were repeated in triplicates, and each group had three disks.

Bacterial morphology

The bacteria with final concentration of 1×10^8 CFU/ml were cultivated on zirconia disks for 24 h prior to SEM observation. After removing the culture medium, the cells were washed three times with sterile PBS solution to remove non-attached cells. The disks were then fixed with 2.5% glutaraldehyde (Solarbio, Beijing, China) overnight at 4 °C, washed three times with PBS buffer, and then dehydrated through a graded series of ethanol (30, 60, 90, 95, 100%, v/v) each for 5 min. Disks were naturally dried, sputter-coated with gold, and imaged by SEM.

LIVE/DEAD staining assay

The LIVE/DEAD BacLight Bacterial Viability Kit (L-7012, Invitrogen, MA, USA) was used to assess the viability of bacterial cells after cultivated 3 h and 24 h on zirconia disks. The staining components A (SYTO 9) and B (propidium iodide) were mixed and diluted with PBS at a volume ratio of 1.5:1000, according to the manufacturer's protocol. After discarding the growth medium, the disks were washed three times with PBS and 300 μ l mixed staining dilution was added to each sample, followed by 15 min incubation at 37 °C in the dark. The stained bacteria were observed using confocal laser scanning microscopy (CLSM; LSM710, Zeiss, Oberkochen, Germany) at 40-fold magnification, where live cells can be observed green-fluorescent and dead cells observed red-fluorescent. Experiments of all four groups were repeated in triplicates, and each group had three disks.

Biofilm staining assay

The crystal violet (CV) assay was performed to determine the total amount of biofilm [43]. The bacteria with final concentration of 1×10^8 CFU/ml were cultivated on zirconia disks for 24 h, 48 h, and 72 h. After the growth medium discarded, wells were washed with PBS and the plates were air-dried. The samples were fixed with 2.5% glutaraldehyde for 20 min

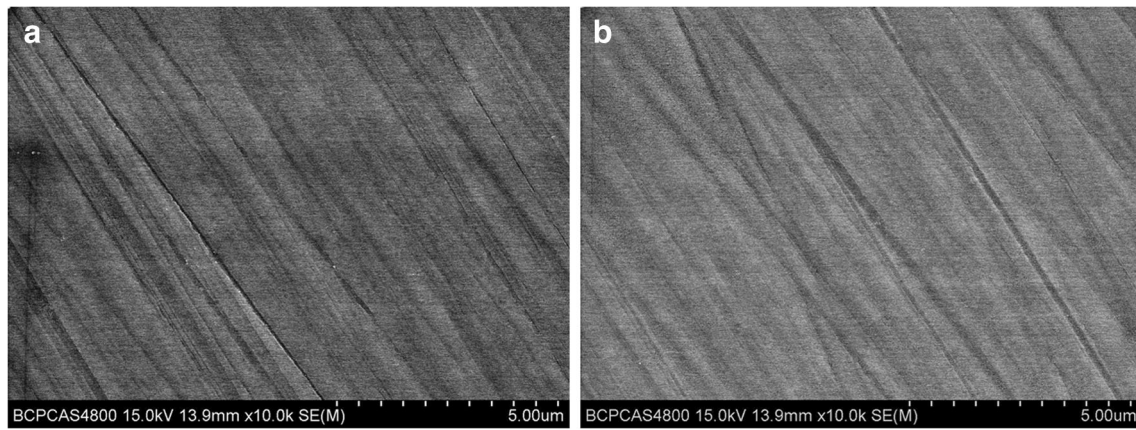


Fig. 3 SEM image of zirconia surfaces. **a** Untreated and **b** Plasma treated for 90 s

at 37 °C, followed by three times washing with PBS and air-dried again. The fixed biofilm was stained using 1% crystal violet solution (Sigma-Aldrich, MO, USA) followed by 10-min incubation at room temperature. The unbound dye was washed with gentle running deionized water, and the bound CV was extracted with absolute ethanol. The amount of biofilm was measured at optical density of 570 nm using microplate reader. Experiments of all four groups were repeated in triplicates, and each group had three disks.

Statistical analysis

The data were expressed as means ± standard deviations. One-way ANOVA test was utilized to determine the level of significance using SPSS software (version 25, IBM, NY, USA) ($\alpha = .05$).

Results

Characterization of the helium AP-DBD jet

In this study, the high-purity helium was used as the plasma-forming gas to produce the low-temperature plasma jet. The chemically reactive species in the plasma jet region is shown

in Fig. 2. It is seen that except for helium atom, there exist hydroxyl free radical ($\cdot\text{OH}$, 307–310 nm), excited oxygen ions (O_2^+ , 427.7 nm), and atomic oxygen (O I, 777.4 nm), which are the so-called reactive oxygen species (ROS), and the reactive nitrogen species (RNS) such as the nitric oxide (NO, 283.0 nm). The production of the ROS and RNS in the plasma jet region is attributed from the strong interactions between the main helium plasma stream and the surrounding air [44]. The 90-s plasma treatment led to a surface temperature increase from 22.1 ± 0.1 to 30.5 ± 0.2 °C.

Surface characteristics

Surface topography

The SEM images of zirconia surface before and after plasma treatment are shown in Fig. 3. With no significant difference observed, all specimens showed a relatively smooth morphology with some typical ground marks and grooves coming from the grinding process.

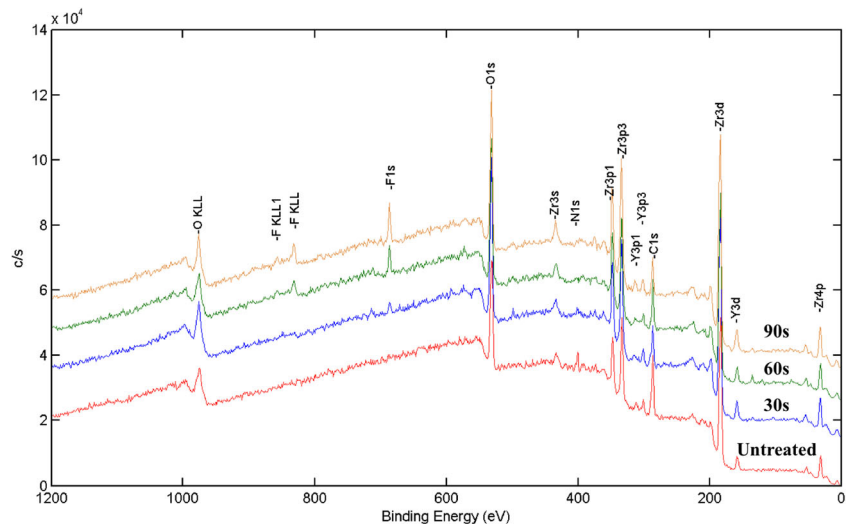
Surface wettability

The surface wettability results are shown in Table 1. The contact angles of the surfaces decreased significantly from 80.89°

Table 1 Surface wettability of zirconia specimen (Values indicated by the same lowercase letters are not significantly different) ($P > .05$)

Group	Untreated	30s	60s	90s
Image				
Water contact angle (°)	80.89 ± 0.51 ^a	63.79 ± 3.52 ^b	43.98 ± 1.25 ^c	25.70 ± 2.06 ^d

Fig. 4 XPS broad spectrum of specimen



to 25.70° after 90-s plasma treatment, showing a more hydrophilic surface created by plasma treatment.

Surface chemistry composition

The XPS analysis of specimens showed peaks of C1s, O1s, N1s, Y3d, and Zr3d (Fig. 4). The atomic percentage of surfaces is shown in Table 2. After the plasma treatment, the percentage of oxygen of all groups increased from 40.06 to over 50%, and the surface C/O ratio decreased. High resolution of oxygen result is shown in Fig. 5. In all plasma-treated groups, there is a peak of 532.5 eV detected, which represents the oxygen in hydroxide state.

Bacterial response

Bacterial adhesion on the plasma-treated surfaces

The adhesion and growth of *S. mutans* and *P. gingivalis* was investigated through MTT assays. As shown in Fig. 6, after 24-h cultivation, the OD result among untreated group, 30 s, 60 s, and 90 s treatment groups have significant difference for *S. mutans* and *P. gingivalis*, suggesting a significant reduction in bacterial adhesion on the plasma-treated surfaces for both strains. The results for 48-h cultivation and 72-h cultivation were in the same trends, indicating that inhibition effect

remained after 72-h cultivation. As treatment time increased, less bacteria were adhered to the material surface.

Bacterial morphology on the plasma-treated surface

To further investigate the bacterial morphology, SEM was utilized (Figs. 7 and 8). A total bacterial load decrease was observed on the plasma-treated surface. In addition, the bacteria on treated surface were more scattered compared with untreated surface, which indicates the reproduction ability of bacteria was interfered after the plasma treatment.

Bacterial viability on plasma-treated surfaces

The viability of bacteria was determined by BacLight LIVE/DEAD assay kit. As shown in Figs. 9 and 10, the viable bacteria cells were stained green while the inviable bacterial cells were stained red. For both strains, after 3-h cultivation, the number of viable bacteria was greater in the untreated group than in the plasma-treated group. As the treatment time increases, the number of viable bacteria decreases: in 90 s treatment group, more red bacteria were observed. The result showed consistency in 24-h cultivation as 3-h ones.

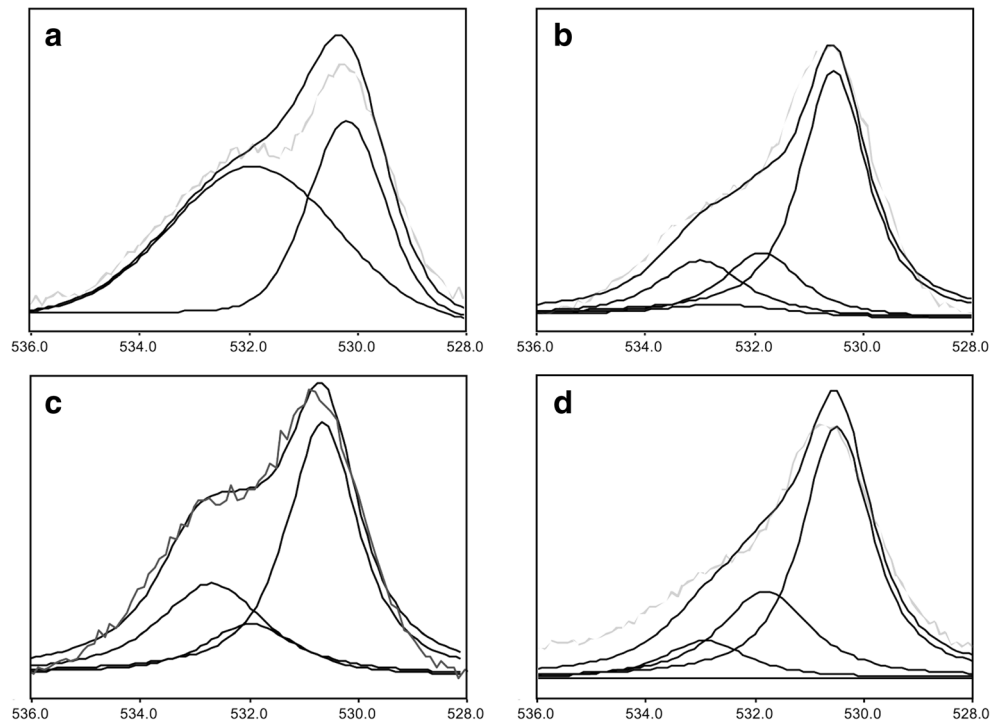
Biofilm formation ability on plasma-treated surfaces

To determine the total biofilm formed on the zirconia surface, crystal violet assays were used. The results of the crystal violet assay are shown in Fig. 11. For *S. mutans*, after 24-h cultivation, the OD result of the untreated group showed significant difference with the treated group. In 30 s, 60 s, and 90 s treatment groups, a low quantity of biofilm was formed. After 48-h cultivation, significant differences can be observed among different groups. As the plasma treatment time increased, the biofilm formation decreased. The same trend can be observed after 72-h cultivation. For *P. gingivalis*, the differences were

Table 2 Atomic percentage of C1s and O1s on specimen surfaces

	C1s (%)	O1s (%)	C/O Ratio
Untreated	41.32	40.06	1.03
30s	25.66	53.36	0.48
60s	29.43	53.60	0.55
90s	26.96	51.32	0.53

Fig. 5 O1s high resolution image (a untreated, b 30 s, c 60 s, d 90 s)



observed among all groups after 24-h cultivation, and the plasma-treated groups had less biofilm formed than the control group. After 48-h and 72-h cultivation, the total biofilm formation of plasma-treated surfaces was significantly less than untreated surface. However, no differences were seen between the 30 s and 60 s treatment groups.

Discussion

The results in this study show that helium CAP jet treatment does not change surface topography of zirconia disks, while creating a hydrophilic surface and could be seen through contact angle tests. Meanwhile, it inhibits the growth of gram-

positive bacteria *Streptococcus mutans* and gram-negative bacteria *Porphyromonas gingivalis* on treated surface.

It is known that surface roughness, surface free energy, and surface chemistry are three key elements that affect material interaction with living cells [12]. In order to enhance host tissue response while eliminating bacteria adhesion, different methods have been investigated, in terms of change of the above characteristics [14, 16, 45]. However, most surface modification methods may change the topography of the materials at the same time, thus making it difficult to be applied in clinic due to unknown complications brought by surface topography change in the long term. In this study, zirconia surface topography remained unchanged after CAP treatment. Based on optical emission spectroscopy and X-ray photoelectron spectroscopy results, the peak of hydroxyl free radical at 307–310 nm

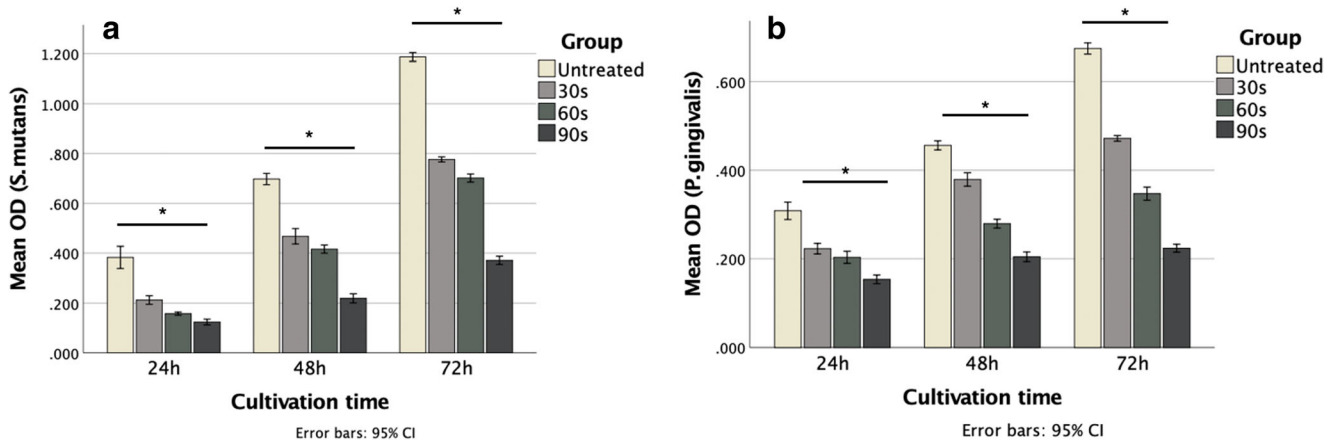


Fig. 6 MTT assay results. Significant difference can be found after 72-h cultivation. **a** *S. mutans*, **b** *P. gingivalis*. *Statistical significance

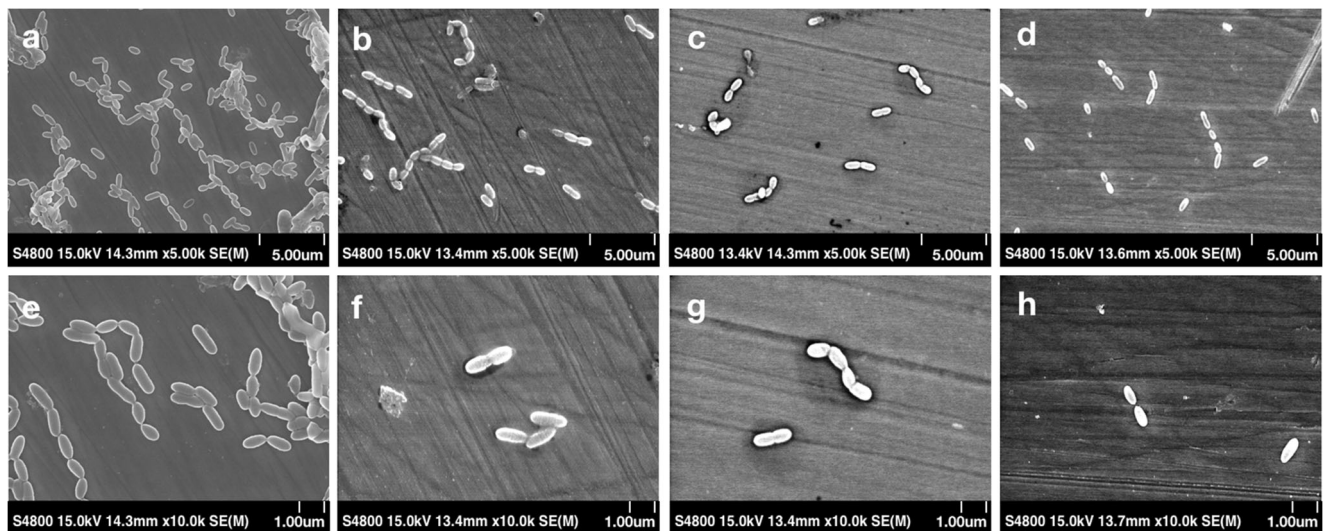


Fig. 7 SEM images of *S. mutans* (a, e untreated, b, f 30 s, c, g 60 s, d, h 90 s, one for 5 k magnification and one for 10 k magnification)

wavelength was detected from the plasma, and the peak of hydroxide with a bonding energy of 532.5 eV was detected in all plasma-treated zirconia surfaces. This indicates that zirconia surface was activated by receiving reactive species from the CAP. The reactive species may be responsible for changing surface chemistry, leading to a hydrophilic surface.

The soft tissue cells, mainly epithelial cells and human gingival fibroblasts, tend to adhere on biomaterial with a smooth and hydrophilic surface [23]. However, microorganisms will also interact with material surface, depending on its surface free energy [46]. There seems to be a contradiction between promoting soft tissue cells and preventing bacterial growth. For example, creating a hydrophilic surface to increase surface free energy on one hand is a viable method to increase tissue cell growth, but on the other hand promotes certain bacterial adhesion. It was reported that most oral bacteria have high surface free energy and thus exhibit higher retention characteristics to hydrophilic surface [47,

48]. However, in this study, plasma treatment did not promote bacterial adhesion and growth on a hydrophilic surface. The results are in accordance with previous studies [35, 49]. The possible reason can be explained with reactive oxygen and nitrogen species, which inhibit the bacteria growth and kill the viable bacteria while lingering on the zirconia surface [50]. The plasma treatment prior to implant abutment placement could also decontaminate the abutment surface. Therefore, in clinical scenario, this method has potential usage not only for preventing infection before implantation, but also for reducing bacterial contamination during the surgery process, making microorganisms less likely to have a head start in the race for the surface.

Human oral cavity consists thousands of bacterial species, which form a sophisticated structure to resist against shear forces, namely biofilm [51]. The biofilm, once formed, is difficult to remove and will cause infection in susceptible population. During early phase of biofilm

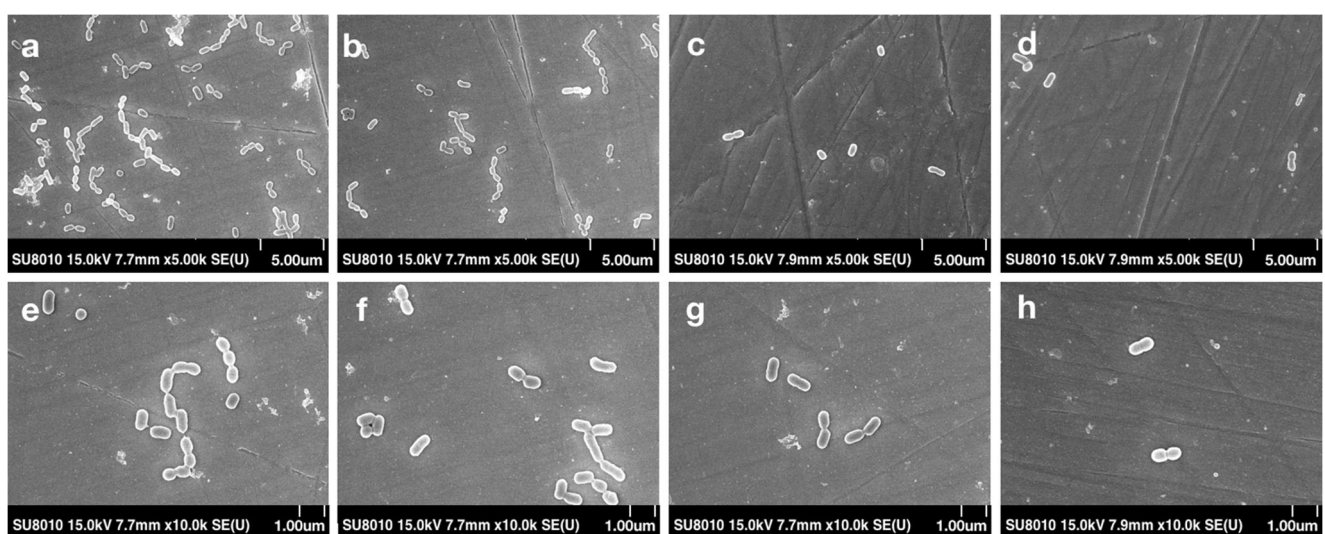


Fig. 8 SEM images of *P. gingivalis* (a, e untreated, b, f 30 s, c, g 60 s, d, h 90 s, one for 5 k magnification and one for 10 k magnification)

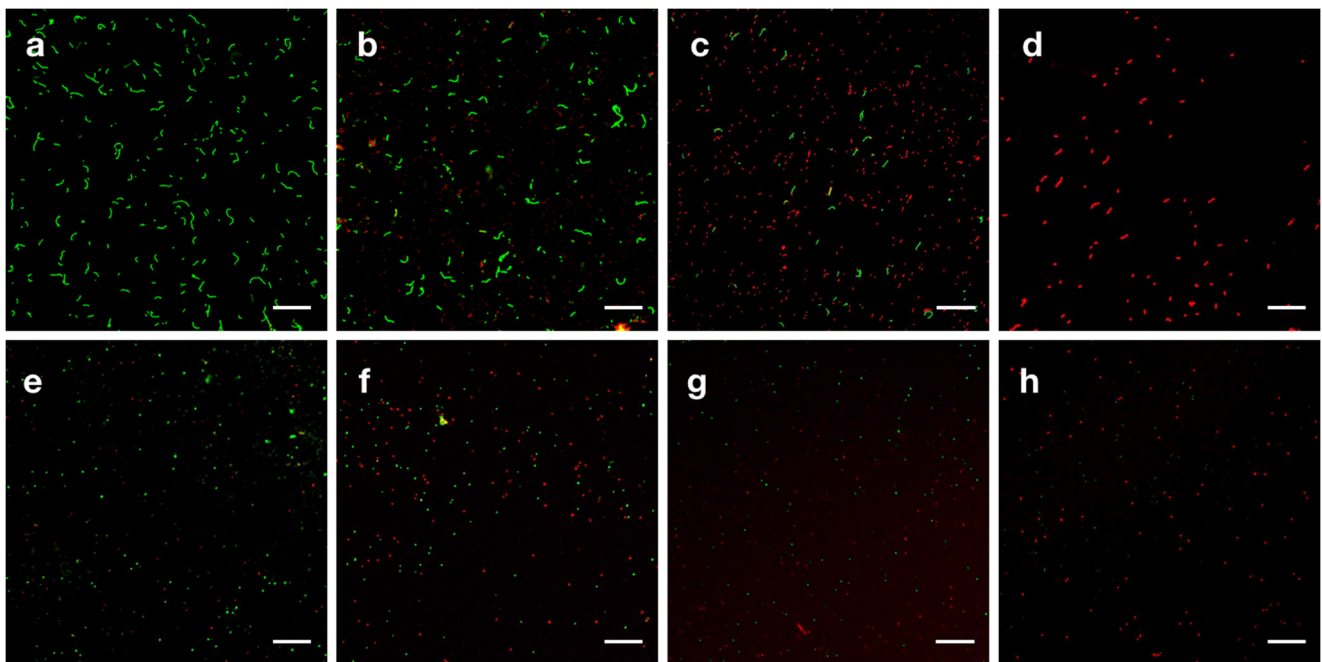


Fig. 9 Images for 3-h LIVE/DEAD assay. **a–d** *S. mutans*, **e–h** *P. gingivalis*. Plasma exposure time: **a, e** untreated, **b, f** 30 s, **c, g** 60 s, **d, h** 90 s. The scale bar is 20 μm

formation, bacteria are mainly Streptococcus species [52]. *S. mutans*, one of the Streptococcus, commonly exist in human oral cavities, and quickly adhere to material surface. Late colonizers such as *P. gingivalis*, a common pathogen for periodontitis, are also found in implant sites in the early stage after material installation [8]. It is believed that patients who suffer from uncontrolled periodontitis are more likely to develop peri-implantitis if

receiving implant treatment [3, 53]. On the other hand, *S. mutans* are gram-positive bacteria which have thick cell walls and consist an identical composition namely peptidoglycan, while gram-negative bacteria, *P. gingivalis*, only have thin cell walls and behave differently in the way of biofilm formation compared with *S. mutans* [54, 55]. Since these two bacteria are different in a large extent yet play important roles in early colonization, they were

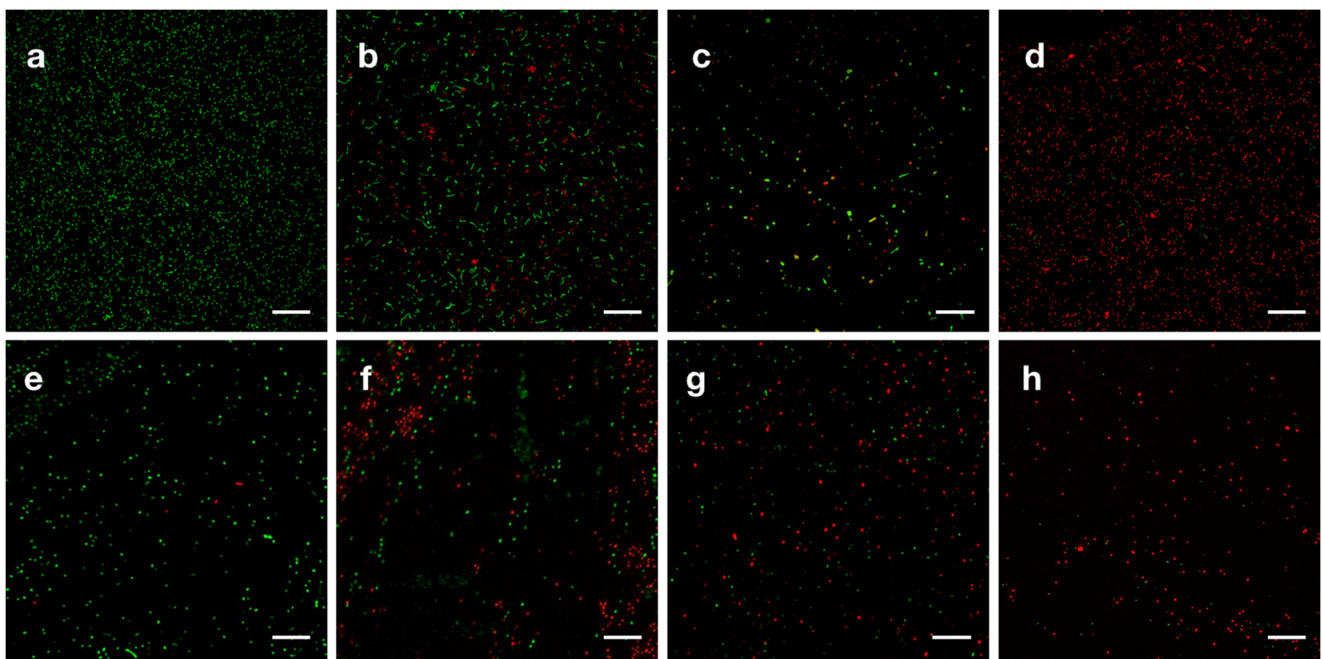


Fig. 10 Images for 24-h LIVE/DEAD assay. **a–d** *S. mutans*, **e–h** *P. gingivalis*. Plasma exposure time: **a, b** untreated, **b, f** 30 s, **c, g** 60 s, **d, h** 90 s. The scale bar is 20 μm

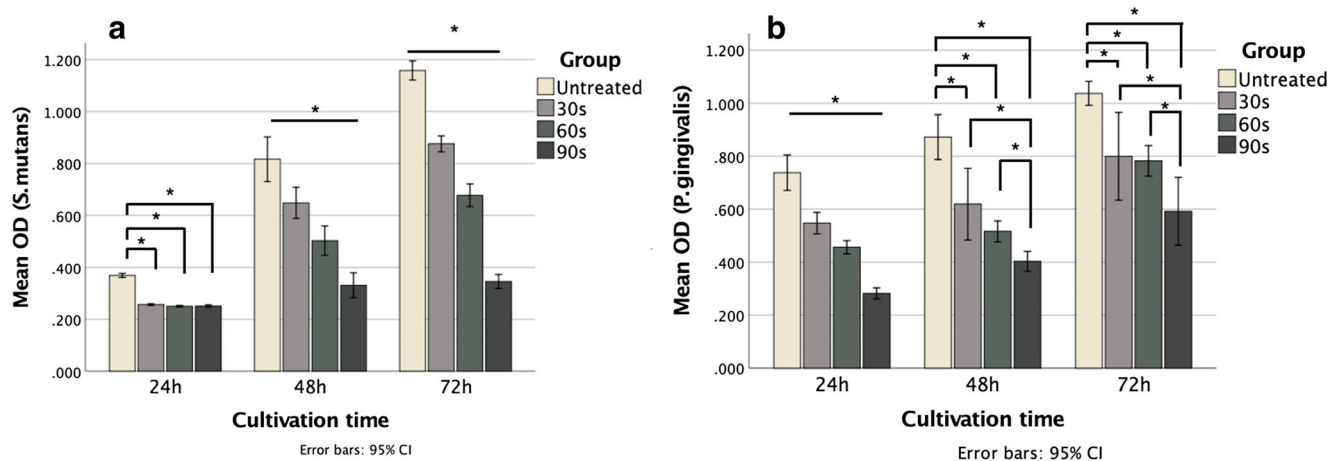


Fig. 11 Crystal violet assay results. Significant difference can be found after 72-h cultivation. **a** *S. mutans*, **b** *P. gingivalis*. *Statistical significance

evaluated in this study. As plasma treatment time increases, bacterial adhesion decreased for both species. The biofilm formation for both stains was also decreased on treated specimens. This could be possibly explained by more reactive species left on the material surface. Interestingly, for *P. gingivalis*, no differences on the biofilm formation were observed between the 30 s and 60 s group after 48 and 72-h cultivation, indicating these two species might have different responses to the same plasma treatment. As the proposed explanation is only hypothetical, and many factors are included in the biofilm formation process, further investigations are needed to define the underlying mechanisms. Moreover, there are researchers indicating differences of sensitivity between gram-positive and gram-negative bacteria, mainly due to their cell wall differences [56]. However, in this study, the trends for two strains are shown in a similar way. Possible explanation could be different experimental design between two studies: this study focuses more on bacterial growth inhibition, while the previous study focuses more on bactericidal efficacy of CAP. The reactive species left on the surface in this study could interact with different microorganisms at a slow rate and finally led to their death.

The cold plasma treatment time will cause different responses on both soft tissue cells and bacteria. From the previous study, CAP treatment for 60 s can enhance biological behavior of human gingival fibroblasts, but treatment for 90 s will suppress the cell behaviors [40]. Taken together with the results of this present study, it is not difficult to infer that there is a best condition where bacteria can be eliminated to the greatest extent while soft tissue cells' behavior can be enhanced. The 60-s plasma treatment group looks promising in meeting both ends but needs more investigation, especially the co-culture experiment with host cells and microorganisms present at the same time. Nevertheless, due to different plasma generation devices and experimental settings, it is rather

difficult to draw a conclusion that suits universally. Even so, CAP effect on living cells shall be similar provided that same amount of reactive species is generated.

Over the results presented in this work, several limitations can be identified. First of all, as the microorganisms interact with acquired pellicles formed minutes after abutment material installation, bacterial inhibition efficacy after CAP treatment should be further evaluated under the presence of saliva coatings. The protein in saliva coating might play a role in the plasma-microorganism interactions. Furthermore, the time-dependent effect of CAP treatment should be further evaluated in order to determine how long this effect lasts. Last but not most important, prior to the clinical usage of plasma-treated zirconia, more studies such as in vitro co-culture studies with mixed oral microbiota and in vivo studies should be performed.

Conclusions

In this study, a simple and effective method was proposed for the surface modification of zirconia abutments. With the limitation of this study, the following conclusions can be drawn:

- (1) The helium CAP jet treatment increases the hydrophilicity of the zirconia abutment material surfaces without changing surface topography. The surface chemistry has been altered after the plasma treatment.
- (2) After the helium CAP jet treatment, bacterial adhesion and growth on the zirconia surfaces was inhibited. The bacterial inhibition was possibly due to the chemically reactive species, such as ROS and RNS, in the CAP jet.

Acknowledgments The authors also thank Dr. Ming-Yue Liu and Dr. Zhen Yang for their support in bacterial culture and bacterial inhibition assays and Dr. Xiao-Ming Zhu for her support in CAP jet analysis. We also thank Dr. Hong Xie for language and grammar review.

Author contributions All the authors contributed to the study conception and design. The interdisciplinary collaborations between dentistry and engineering physics requires authors from different institutions work together. The experimental protocol was provided by He-Ping Li and Jian-Guo Tan. Material preparation, data collection, and analysis regarding dentistry field were performed by Yang Yang¹, Miao Zheng, and Yang Yang³. Material preparation, data collection, and analysis regarding engineering physics field were performed by Jing Li and Yong-Fei Su. The first draft of the manuscript was written by Yang Yang¹ and Miao Zheng, and all the authors commented on previous versions of the manuscript. All the authors read and approved the final manuscript.

Funding information The work was supported by the National Natural Science Foundation of China (No. 81801013 and No. 81701003).

Compliance with ethical standards

Conflict of interest The authors declare that they have no conflict of interest.

Ethical approval This article does not contain any studies with human participants or animals performed by any of the authors.

Informed consent For this type of study, formal consent is not required.

References

- Berglundh T, Lindhe J, Ericsson I, Marinello CP, Liljenberg B, Thomsen P (1991) The soft tissue barrier at implants and teeth. *Clin Oral Implants Res* 2:81–90. <https://doi.org/10.1034/j.1600-0501.1991.020206.x>
- Ivanovski S, Lee R (2018) comparison of peri-implant and periodontal marginal soft tissues in health and disease. *Periodontol* 2000 76:116–130. <https://doi.org/10.1111/prd.12150>
- Renvert S, Quirynen M (2015) Risk indicators for peri-implantitis. A narrative review. *Clin Oral Implants Res* 26:15–44. <https://doi.org/10.1111/clr.12636>
- Rakic M, Galindo-Moreno P, Monje A, Radovanovic S, Wang H-L, Cochran D, Sculean A, Canullo L (2017) How frequent does peri-implantitis occur? A systematic review and meta-analysis. *Clin Oral Investig* 22:1805–1816. <https://doi.org/10.1007/s00784-017-2276-y>
- Wang Y, Zhang Y, Miron RJ (2016) Health, maintenance, and recovery of soft tissues around implants. *Clin Implant Dent R* 18: 618–634. <https://doi.org/10.1111/cid.12343>
- Salvi GE, Bosshardt DD, Lang NP, Abrahamsson I, Berglundh T, Lindhe J, Ivanovski S, Donos N (2015) Temporal sequence of hard and soft tissue healing around titanium dental implants. *Periodontol* 68:135–152. <https://doi.org/10.1111/prd.12054>
- Gristina A (1987) Biomaterial-centered infection: microbial adhesion versus tissue integration. *Science* 237:1588–1595. <https://doi.org/10.1126/science.3629258>
- Fürst MM, Salvi GE, Lang NP, Persson GR (2007) Bacterial colonization immediately after installation on oral titanium implants. *Clin Oral Implants Res* 18:501–508. <https://doi.org/10.1111/j.1600-0501.2007.01381.x>
- Subbiahdoss G, Grijpma DW, van der Mei HC, Busscher HJ, Kuijper R (2010) Microbial biofilm growth versus tissue integration on biomaterials with different wettabilities and a polymer-brush coating. *J Biomed Mater Res A* 94:533–538. <https://doi.org/10.1002/jbm.a.32731>
- Sculean A, Gruber R, Bosshardt DD (2014) Soft tissue wound healing around teeth and dental implants. *J Clin Periodontol* 41: S6–S22. <https://doi.org/10.1111/jcpe.12206>
- Tomasi C, Tessarolo F, Caola I, Piccoli F, Wennström JL, Nollo G, Berglundh T (2016) Early healing of peri-implant mucosa in man. *J Clin Periodontol* 43:816–824. <https://doi.org/10.1111/jcpe.12591>
- Han A, Tsoi JKH, Rodrigues FP, Leprince JG, Palin WM (2016) Bacterial adhesion mechanisms on dental implant surfaces and the influencing factors. *Int J Adhes Adhes* 69:58–71. <https://doi.org/10.1016/j.jadhadh.2016.03.022>
- Socransky SS, Haffajee AD, Cugini MA, Smith C, Kent RL Jr (1998) Microbial complexes in subgingival plaque. *J Clin Periodontol* 25:134–144. <https://doi.org/10.1111/j.1600-051X.1998.tb02419.x>
- Werner S, Huck O, Frisch B, Vautier D, Elkaim R, Voegel J-C, Brunel G, Tenenbaum H (2009) The effect of microstructured surfaces and laminin-derived peptide coatings on soft tissue interactions with titanium dental implants. *Biomaterials* 30:2291–2301. <https://doi.org/10.1016/j.biomaterials.2009.01.004>
- Teughels W, Van Assche N, Sliepen I, Quirynen M (2006) Effect of material characteristics and/or surface topography on biofilm development. *Clin Oral Implants Res* 17:68–81. <https://doi.org/10.1111/j.1600-0501.2006.01353.x>
- Larsson A, Andersson M, Wigren S, Pivodic A, Flynn M, Nannmark U (2015) Soft tissue integration of hydroxyapatite-coated abutments for bone conduction implants. *Clin Implant Dent R* 17:e730–e735. <https://doi.org/10.1111/cid.12304>
- Sanz-Martín I, Sanz-Sánchez I, Carrillo de Albornoz A, Figuero E, Sanz M (2018) Effects of modified abutment characteristics on peri-implant soft tissue health: a systematic review and meta-analysis. *Clin Oral Implants Res* 29:118–129. <https://doi.org/10.1111/clr.13097>
- Fretwurst T, Nelson K, Tarnow DP, Wang HL, Giannobile WV (2018) Is metal particle release associated with peri-implant bone destruction? An emerging concept. *J Dent Res* 97:259–265. <https://doi.org/10.1177/0022034517740560>
- Lorenz J, Giulini N, Hölscher W, Schwiertz A, Schwarz F, Sader R (2019) Prospective controlled clinical study investigating long-term clinical parameters, patient satisfaction, and microbial contamination of zirconia implants. *Clin Implant Dent R* 21:263–271. <https://doi.org/10.1111/cid.12720>
- Blatz MB, Bergler M, Holst S, Block MS (2009) Zirconia abutments for single-tooth implants—rationale and clinical guidelines. *J Oral Maxillofac Surg* 67:74–81. <https://doi.org/10.1016/j.joms.2009.07.011>
- Al-Radha ASD, Dymock D, Younes C, O'Sullivan D (2012) Surface properties of titanium and zirconia dental implant materials and their effect on bacterial adhesion. *J Dent* 40:146–153. <https://doi.org/10.1016/j.jdent.2011.12.006>
- Hashim D, Cionca N, Courvoisier DS, Mombelli A (2016) A systematic review of the clinical survival of zirconia implants. *Clin Oral Investig* 20:1403–1417. <https://doi.org/10.1007/s00784-016-1853-9>
- Yang Y, Zhou J, Liu X, Zheng M, Yang J, Tan J (2015) Ultraviolet light-treated zirconia with different roughness affects function of human gingival fibroblasts in vitro: the potential surface modification developed from implant to abutment. *J Biomed Mater Res B* 103:116–124. <https://doi.org/10.1002/jbm.b.33183>
- Liu M, Zhou J, Yang Y, Zheng M, Yang J, Tan J (2015) Surface modification of zirconia with polydopamine to enhance fibroblast response and decrease bacterial activity in vitro: a potential technique for soft tissue engineering applications. *Colloids Surf B: Biointerfaces* 136:74–83. <https://doi.org/10.1016/j.colsurfb.2015.06.047>

25. Abdallah M-N, Badran Z, Ciobanu O, Hamdan N, Tamimi F (2017) Strategies for optimizing the soft tissue seal around osseointegrated implants. *Adv Healthc Mater*:6. <https://doi.org/10.1002/adhm.201700549>
26. Li H-P, Zhang X-F, Zhu X-M, Zheng M, Liu S-F, Qi X, Wang K-P, Chen J, Xi X-Q, Tan J-G, Ostrikov K (2017) Translational plasma stomatology: applications of cold atmospheric plasmas in dentistry and their extension. *High Voltage* 2:188–199. <https://doi.org/10.1049/hve.2017.0066>
27. Garcia B, Camacho F, Peñarrocha D, Tallarico M, Perez S, Canullo L (2017) Influence of plasma cleaning procedure on the interaction between soft tissue and abutments: a randomized controlled histologic study. *Clin Oral Implants Res* 28:1269–1277. <https://doi.org/10.1111/clr.12953>
28. Canullo L, Tallarico M, Botticelli D, Alccayhuaman KAA, Martins Neto EC, Xavier SP (2018) Hard and soft tissue changes around implants activated using plasma of argon: a histomorphometric study in dog. *Clin Oral Implants Res* 29:389–395. <https://doi.org/10.1111/clr.13134>
29. Canullo L, Peñarrocha D, Clementini M, Iannello G, Micarelli C (2015) Impact of plasma of argon cleaning treatment on implant abutments in patients with a history of periodontal disease and thin biotype: radiographic results at 24-month follow-up of a RCT. *Clin Oral Implants Res* 26:8–14. <https://doi.org/10.1111/clr.12290>
30. Liao X, Liu D, Xiang Q, Ahn J, Chen S, Ye X, Ding T (2017) Inactivation mechanisms of non-thermal plasma on microbes: a review. *Food Control* 75:83–91. <https://doi.org/10.1016/j.foodcont.2016.12.021>
31. Lunov O, Zablotskii V, Churpita O, Jäger A, Polívka L, Syková E, Dejneka A, Kubinová Š (2016) The interplay between biological and physical scenarios of bacterial death induced by non-thermal plasma. *Biomaterials* 82:71–83. <https://doi.org/10.1016/j.biomaterials.2015.12.027>
32. Gilmore BF, Flynn PB, O'Brien S, Hickok N, Freeman T, Bourke P (2018) Cold plasmas for biofilm control: opportunities and challenges. *Trends Biotechnol* 36:627–638. <https://doi.org/10.1016/j.tibtech.2018.03.007>
33. Lee JH, Jeong WS, Seo SJ, Kim HW, Kim KN, Choi EH, Kim KM (2017) Non-thermal atmospheric pressure plasma functionalized dental implant for enhancement of bacterial resistance and osseointegration. *Dent Mater* 33:257–270. <https://doi.org/10.1016/j.dental.2016.11.011>
34. Canullo L, Genova T, Wang HL, Carossa S, Mussano F (2017) Plasma of argon increases cell attachment and bacterial decontamination on different implant surfaces. *Int J Oral Maxillofac Implants* 32:1315–1323. <https://doi.org/10.11607/jomi.5777>
35. Genova T, Pesce P, Mussano F, Tanaka K, Canullo L (2019) The influence of bone-graft bio-functionalization with plasma of argon on bacterial contamination. *J Biomed Mater Res A* 107:67–70. <https://doi.org/10.1002/jbm.a.36531>
36. Pistilli R, Genova T, Canullo L, Faga MG, Terlizzi ME, Griboaud G, Mussano F (2018) Effect of bioactivation on traditional surfaces and zirconium nitride: adhesion and proliferation of preosteoblastic cells and bacteria. *Int J Oral Maxillofac Implants* 33:1247–1254. <https://doi.org/10.11607/jomi.6654>
37. Lee MJ, Kwon JS, Jiang HB, Choi EH, Park G, Kim KM (2019) The antibacterial effect of non-thermal atmospheric pressure plasma treatment of titanium surfaces according to the bacterial wall structure. *Sci Rep* 9:1938. <https://doi.org/10.1038/s41598-019-39414-9>
38. Canullo L, Genova T, Tallarico M, Gautier G, Mussano F, Botticelli D (2016) Plasma of argon affects the earliest biological response of different implant surfaces: an in vitro comparative study. *J Dent Res* 95:566–573. <https://doi.org/10.1177/0022034516629119>
39. Henningsen A, Smeets R, Hartjen P, Heinrich O, Heuberger R, Heiland M, Precht C, Cacaci C (2018) Photofunctionalization and non-thermal plasma activation of titanium surfaces. *Clin Oral Investig* 22:1045–1054. <https://doi.org/10.1007/s00784-017-2186-z>
40. Zheng M, Yang Y, Liu XQ, Liu MY, Zhang XF, Wang X, Li HP, Tan JG (2015) Enhanced biological behavior of in vitro human gingival fibroblasts on cold plasma-treated zirconia. *PLoS One* 10:e0140278. <https://doi.org/10.1371/journal.pone.0140278>
41. Li D, Li G, Li J, Liu Z-Q, Zhang X, Zhang Y, Li H-P (2019) Promotion of wound healing of genetic diabetic mice treated by a cold atmospheric plasma jet. *IEEE T Plasma Sci* 47:4848–4860. <https://doi.org/10.1109/tps.2019.2928320>
42. Wu T, Hu W, Guo L, Finnegan M, Bradshaw DJ, Webster P, Loewy ZG, Zhou X, Shi W, Lux R (2013) Development of a new model system to study microbial colonization on dentures. *J Prosthodont* 22:344–350. <https://doi.org/10.1111/jopr.12002>
43. Wang G, Feng H, Hu L, Jin W, Hao Q, Gao A, Peng X, Li W, Wong K-Y, Wang H, Li Z, Chu PK (2018) An antibacterial platform based on capacitive carbon-doped TiO₂ nanotubes after direct or alternating current charging. *Nat Commun* 9:2055. <https://doi.org/10.1038/s41467-018-04317-2>
44. Li J, Guo H, Zhang X-F, Li H-P (2018) Numerical and experimental studies on the interactions between the radio-frequency glow discharge plasma jet and the shielding gas at atmosphere. *IEEE Trans Plasma Sci* 46:2766–2775. <https://doi.org/10.1109/tps.2018.2852945>
45. Calliess T, Bartsch I, Haupt M, Reebmann M, Schwarze M, Stiesch M, Pfaffenroth C, Sluszniaik M, Dempwolf W, Menzel H, Witte F, Willbold E (2016) In vivo comparative study of tissue reaction to bare and antimicrobial polymer coated transcutaneous implants. *Mater Sci Eng C* 61:712–719. <https://doi.org/10.1016/j.msec.2015.12.095>
46. Quirynen M, Bollen CM (1995) The influence of surface roughness and surface-free energy on supra- and subgingival plaque formation in man. A review of the literature. *J Clin Periodontol* 22:1–14. <https://doi.org/10.1111/j.1600-051X.1995.tb01765.x>
47. Uyen M (1985) Surface free energies of oral streptococci and their adhesion to solids. *FEMS Microbiol Lett* 30:103–106. <https://doi.org/10.1111/j.1574-6968.1985.tb00993.x>
48. Weerkamp AH, Quirynen M, Marechal M, Van Der Mei HC, Steenberghe DV, Busscher HJ (2009) The role of surface free energy in the early in vivo formation of dental plaque on human enamel and polymeric substrata. *Microb Ecol Health Dis* 2:11–18. <https://doi.org/10.3109/08910608909140196>
49. Rochford ETJ, Subbiahdoss G, Moriarty TF, Poulsson AHC, van der Mei HC, Busscher HJ, Richards RG (2014) An in vitro investigation of bacteria-osteoblast competition on oxygen plasma-modified PEEK. *J Biomed Mater Res A* 102:4427–4434. <https://doi.org/10.1002/jbm.a.35130>
50. Mai-Prochnow A, Murphy AB, McLean KM, Kong MG, Ostrikov K (2014) Atmospheric pressure plasmas: infection control and bacterial responses. *Int J Antimicrob Agents* 43:508–517. <https://doi.org/10.1016/j.ijantimicag.2014.01.025>
51. Costerton J (1999) Introduction to biofilm. *Int J Antimicrob Agents* 11:217–221. [https://doi.org/10.1016/s0924-8579\(99\)00018-7](https://doi.org/10.1016/s0924-8579(99)00018-7)
52. Marsh PD, Bradshaw DJ (1995) Dental plaque as a biofilm. *J Ind Microbiol* 15:169–175. <https://doi.org/10.1007/BF01569822>
53. Jordan RP, Marsh L, Ayre WN, Jones Q, Parkes M, Austin B, Sloan AJ, Waddington RJ (2016) An assessment of early colonisation of implant-abutment metal surfaces by single species and co-cultured bacterial periodontal pathogens. *J Dent* 53:64–72. <https://doi.org/10.1016/j.jdent.2016.07.013>

54. Tu Y, Ling X, Chen Y, Wang Y, Zhou N, Chen H (2017) Effect of *S. mutans* and *S. sanguinis* on growth and adhesion of *P. gingivalis* and their ability to adhere to different dental materials. *Med Sci Monit* 23:4539–5445. <https://doi.org/10.12659/MSM.904114>
55. Meza-Siccha AS, Aguilar-Luis MA, Silva-Caso W, Mazulis F, Barragan-Salazar C, Del Valle-Mendoza J (2019) In vitro evaluation of bacterial adhesion and bacterial viability of *Streptococcus mutans*, *Streptococcus sanguinis*, and *Porphyromonas gingivalis* on the abutment surface of titanium and zirconium dental implants. *Int J Dent* 2019:4292976. <https://doi.org/10.1155/2019/4292976>
56. Mai-Prochnow A, Clauson M, Hong J, Murphy AB (2016) Gram positive and gram negative bacteria differ in their sensitivity to cold plasma. *Sci Rep* 6:38610. <https://doi.org/10.1038/srep38610>

Publisher's note Springer Nature remains neutral with regard to jurisdictional claims in published maps and institutional affiliations.